

# Ulinastatin suppresses lipopolysaccharide-induced prostaglandin E<sub>2</sub> synthesis and nitric oxide production through the downregulation of nuclear factor- $\kappa$ B in BV2 mouse microglial cells

YUN-HEE SUNG<sup>1</sup>, MAL-SOON SHIN<sup>2</sup>, IL-GYU KO<sup>2</sup>, SUNG-EUN KIM<sup>2</sup>,  
CHANG-JU KIM<sup>2</sup>, HYUN-JONG AHN<sup>3</sup>, HYE-SUN YOON<sup>4</sup> and BONG-JAE LEE<sup>5</sup>

<sup>1</sup>Department of Physical Therapy, Kyungnam University, Changwon 631-701; Departments of <sup>2</sup>Physiology and <sup>3</sup>Microbiology, Kyung Hee University College of Medicine, Seoul 130-701; <sup>4</sup>Department of Pediatrics, Eulji General Hospital, Eulji University School of Medicine, Seoul 139-872; <sup>5</sup>Department of Anesthesiology and Pain Medicine, Kang Dong Kyung Hee Hospital, Kyung Hee University College of Medicine, Seoul 134-890, Republic of Korea

Received January 3, 2013; Accepted March 15, 2013

DOI: 10.3892/ijmm.2013.1322

**Abstract.** Ulinastatin is an intrinsic serine-protease urinary trypsin inhibitor that can be extracted and purified from human urine. Urinary trypsin inhibitors are widely used to treat patients with acute inflammatory disorders, such as shock and pancreatitis. However, although the anti-inflammatory activities of urinary trypsin inhibitors have been investigated, the mechanisms underlying their actions are not yet fully understood. In the present study, we evaluated the effect of ulinastatin on lipopolysaccharide (LPS)-induced inflammation in relation with nuclear factor- $\kappa$ B (NF- $\kappa$ B) activation using BV2 mouse microglial cells. To accomplish this, we performed a 3-(4,5-dimethylthiazol-2-yl)-2,5-diphenyltetrazolium bromide (MTT) assay, reverse transcription-polymerase chain reaction (RT-PCR), western blot analysis, electrophoretic mobility gel shift assay (EMSA), prostaglandin E<sub>2</sub> (PGE<sub>2</sub>) immunoassay and nitric oxide (NO) detection. The results demonstrated that ulinastatin suppressed PGE<sub>2</sub> synthesis and NO production by inhibiting the LPS-induced mRNA and protein expression of cyclooxygenase-2 (COX-2) and inducible NO synthase (iNOS) in BV2 mouse microglial cells. Ulinastatin suppressed the activation of NF- $\kappa$ B in the nucleus. These findings demonstrate that ulinastatin exerts analgesic and anti-inflammatory effects

that possibly occur via the suppression of COX-2 and iNOS expression through the downregulation of NF- $\kappa$ B activity.

## Introduction

Microglial cells, which are regarded as the most important immune cells in the central nervous system (CNS), are activated by brain injuries. Following activation by bacterial toxins, microglial cells secrete a wide range of inflammatory mediators, such as tumor necrosis factor- $\alpha$  (TNF- $\alpha$ ), interleukin (IL)-1 $\beta$ , nitric oxide (NO) and prostanoids (1,2).

Lipopolysaccharide (LPS) activates microglial cells and plays vital roles in the pathogenesis of inflammatory responses by inducing the production of inflammatory mediators (3,4). TNF- $\alpha$  and IL-1 $\beta$  are the most important mediators, and they are known to be secreted during the early phase of inflammatory disease (5).

Prostaglandin E<sub>2</sub> (PGE<sub>2</sub>), which is one of the most prominent prostanoids produced by astrocytes and microglia that have been exposed to noxious stimuli (6,7), is produced by the conversion of arachidonic acid by cyclooxygenase (COX). There are 2 isoforms of COX, COX-1 and COX-2. COX-2 is expressed by pro-inflammatory mediators and mitogenic stimuli (8).

NO is an important physiological messenger and effector molecule in a number of biological systems, including immunological, neuronal and cardiovascular tissues (9). NO is endogenously generated from L-arginine by NO synthase (NOS). There are 3 types of NOS, endothelial NOS (eNOS), neuronal NOS (nNOS) and inducible NOS (iNOS). Of these, iNOS plays an important role in inflammation and host-defense responses (10).

Nuclear factor- $\kappa$ B (NF- $\kappa$ B) regulates the expression of genes involved in cellular proliferation, inflammatory responses and cell adhesion (8,11). In unstimulated cells, NF- $\kappa$ B is held in the cytoplasm by inhibitory I $\kappa$ B protein (I $\kappa$ B). The activation of NF- $\kappa$ B is then induced by the phosphorylation, ubiquitina-

---

*Correspondence to:* Professor Bong-Jae Lee, Department of Anesthesiology and Pain Medicine, Kang Dong Kyung Hee Hospital, Kyung Hee University College of Medicine, 892 Dongnam-ro, Gangdong-gu, Seoul 134-727, Republic of Korea  
E-mail: lbj8350@naver.com

**Key words:** ulinastatin, lipopolysaccharide, prostaglandin E<sub>2</sub>, nitric oxide, nuclear factor- $\kappa$ B

tion and proteasome-mediated degradation of the I $\kappa$ B protein. Following activation, NF- $\kappa$ B undergoes nuclear translocation and DNA binding (12).

Urinary trypsin inhibitors are widely used for the treatment of patients with acute inflammatory disorders, such as pancreatitis (13), septic shock (14), hemorrhagic shock (15) and ischemia-reperfusion injury (16,17). Additionally, urinary trypsin inhibitors are known to ameliorate the enhanced production of pro-inflammatory molecules (18). Ulinastatin is one of the urinary trypsin inhibitors and is an intrinsic serine-protease inhibitor that can be extracted and purified from human urine (19). Ulinastatin has been shown to decrease the occurrence of coronary artery lesions in patients with acute Kawasaki disease by the suppression of neutrophils (20) and to reduce LPS-induced pulmonary injury (21). Diverse effects of ulinastatin have been documented; however, the mechanisms underlying the anti-inflammatory activity of ulinastatin are not yet fully understood.

In the present study, we investigated the effect of ulinastatin on LPS-induced inflammation in relation with NF- $\kappa$ B activation. To accomplish this, we used a 3-(4,5-dimethylthiazol-2-yl)-2,5-diphenyltetrazolium bromide (MTT) assay, reverse transcription-polymerase chain reaction (RT-PCR), western blot analysis, electrophoretic mobility gel shift assay (EMSA), PGE<sub>2</sub> immunoassay, and NO detection in BV2 mouse microglial cells.

## Materials and methods

**Cell culture.** BV2 mouse microglial cells were cultured in Dulbecco's modified Eagle's Medium (DMEM; Gibco BRL, Grand Island, NY, USA) supplemented with 10% heat-inactivated fetal bovine serum (FBS; Gibco BRL) at 37°C under 5% CO<sub>2</sub>-95% O<sub>2</sub> in a humidified cell incubator. The cells were then plated onto culture dishes at a density of 2x10<sup>4</sup> cells/cm<sup>2</sup> 24 h prior to drug treatments.

**MTT cytotoxicity assay.** BV2 mouse microglial cells were grown in 100  $\mu$ l of culture medium per well in 96-well plates. Ulinastatin was purchased from Wakamoto Pharmaceutical Co., Ltd. (Tokyo, Japan). To determine the cytotoxicity of ulinastatin, cells were treated with ulinastatin at concentrations of 1, 10, 100, 1,000 and 10,000 U/ml for 24 h. The cells in the control group were left untreated. After incubation, 10  $\mu$ l of MTT labeling reagent containing 5 mg/ml MTT in phosphate-buffered saline were added to each well, and the plates were then incubated for an additional 2 h. Subsequently, 100  $\mu$ l of solubilization solution containing 10% sodium dodecyl sulfate (SDS) in 0.01 M hydrochloric acid were added to each well, after which the cells were incubated for a further 12 h. The absorbance was then measured using a microtiter plate reader (Bio-Tek, Winooski, VT, USA) at a test wavelength of 595 nm and a reference wavelength of 690 nm. The optical density (OD) was then calculated as the difference between the absorbance at the reference wavelength and that of the test wavelength. The percentage viability was then calculated as follows: (OD of drug-treated sample/control OD) x100.

**RNA isolation and RT-PCR.** RT-PCR was conducted to determine the mRNA expression of COX-2 and iNOS. Briefly,

total RNA was isolated from the BV2 mouse microglial cells using RNeasy<sup>TM</sup> B (Tel-Test Inc., Friendswood, TX, USA). Subsequently, 2  $\mu$ g of RNA and 2  $\mu$ l of random hexamers (Promega, Madison, WI, USA) were combined, after which the mixture was heated at 65°C for 15 min. A total of 1  $\mu$ l of AMV reverse transcriptase (Promega), 5  $\mu$ l of 2.5 mM dNTP (Promega), 0.5  $\mu$ l of RNasin (Promega) and 8  $\mu$ l of 5X AMV RT buffer (Promega) were then added to the mixture, which was then brought up to a final volume of 40  $\mu$ l using diethylpyrocabonate (DEPC)-treated water. The reaction mixture was then incubated at 42°C for 2 h.

PCR amplification was performed in a reaction mixture with a final volume of 40  $\mu$ l that contained 1  $\mu$ l of the appropriate cDNA, 0.5  $\mu$ l of each set of primers at a concentration of 10 pM, 4  $\mu$ l of 10X RT buffer, 1  $\mu$ l of 2.5 mM dNTP and 0.2 U of Taq DNA polymerase (Takara, Shiga, Japan). The primers used to amplify COX-2 were 5'-CCAGATGCTATCTTTGG GGAGAC-3' (a 23-mer sense oligonucleotide) and 5'-CTTGCA TTGATGGTGGCTG-3' (a 19-mer antisense oligonucleotide). The primers used to amplify iNOS were 5'-CAAGAGTTTGA CCAGAGGACC-3' (a 21-mer sense oligonucleotide) and 5'-TGGAACCACTCGTACTTGGGA-3' (a 21-mer antisense oligonucleotide). Finally, to amplify *cyclophilin* as the internal control, the primer sequences were 5'-ACCCACCGTGTTC TTCGAC-3' (a 20-mer sense oligonucleotide) and 5'-CATTTG CCATGGACAAGATG-3' (a 20-mer antisense oligonucleotide).

To amplify the COX-2 and iNOS genes, PCR was conducted using a PTC-0150 MiniCycler (Bio-Rad, Hercules, CA, USA) subjecting the reaction mixture to the following conditions: initial denaturation at 94°C for 5 min, followed by 32 cycles of denaturation at 94°C for 30 sec, annealing at 60°C for 30 sec and extension at 72°C for 45 sec, with a final extension at 72°C for 10 min. For *cyclophilin*, PCR was conducted under same conditions, except only 25 amplification cycles were conducted.

**Preparation of whole cell extract.** To prepare the whole cell extract, cells were incubated in ice-cold whole cell lysate buffer that contained 50 mM HEPES (pH 7.5), 150 mM NaCl, 10% glycerol, 1% Triton X-100, 1.5 mM magnesium chloride hexahydrate, 1 mM ethyleneglycol-bis-( $\beta$ -aminoethyl ether)-N,N'-tetraacetic acid (EGTA), 1 mM phenylmethylsulfonyl fluoride (PMSF), 2  $\mu$ g/ml leupeptin, 1  $\mu$ g/ml pepstatin, 1 mM sodium orthovanadate and 100 mM sodium fluoride (NaF) for 15 min. The cells were then centrifuged at 14,000 rpm for 15 min at 4°C, and the supernatant was stored.

**Preparation of nuclear and cytosolic extracts.** The cells were collected and suspended in hypotonic buffer [10 mM HEPES, pH 7.9, 1.5 mM MgCl<sub>2</sub>, 10 mM potassium chloride (KCl), 0.2 mM PMSF, 0.5 mM dithiothreitol (DTT) and 10  $\mu$ g/ml aprotinin], after which they were incubated on ice for 10 min. The cells were then lysed by the addition of 0.1% Nonidet P-40 and vigorous vortexing for 10 sec. The cells were then centrifuged at 4,000 rpm for 5 min at 4°C, after which the supernatants containing protein were collected. The pellets acquired from the cytosolic protein extraction were then resuspended in high salt buffer (20 mM HEPES, pH 7.9, 25% glycerol, 400 mM KCl, 1.5 mM MgCl<sub>2</sub>, 0.2 mM EDTA, 0.5 mM DTT, 1 mM NaF and 1 mM sodium orthovanadate).

Finally, the cells were centrifuged at 14,000 rpm for 5 min at 4°C, and the supernatants were stored.

**Western blot analysis.** Whole protein extract was used to evaluate the protein expression of COX-2 and iNOS. In addition, cytosolic extract was used for the detection of IκB-α, while nuclear extract was used for the detection of NF-κB (p65) protein expression. Prior to analysis, the protein concentrations were measured using a Bio-Rad colorimetric protein assay kit (Bio-Rad). Subsequently, 40 μg of protein were separated on SDS-polyacrylamide gels and then transferred onto a nitrocellulose membrane (Schleicher & Schuell GmbH, Dassel, Germany). Goat COX-2 antibody (1:1,000; Santa Cruz Biotechnology, Santa Cruz, CA, USA), rabbit iNOS antibody (1:500; Santa Cruz Biotechnology), rabbit NF-κB (p65) antibody (1:500; Santa Cruz Biotechnology) and rabbit IκB-α antibody (1:500; Santa Cruz Biotechnology) were used as the primary antibodies. Horseradish peroxidase-conjugated anti-goat antibody (1:4,000; Santa Cruz Biotechnology) was used to probe for COX-2. Anti-rabbit antibody (1:2,000; Vector Laboratories, Burlingame, CA, USA) was used as the secondary antibody for iNOS, NF-κB (p65) and IκB-α. Bands were detected using the enhanced chemiluminescence (ECL) detection system (Santa Cruz Biotechnology).

**EMSA.** EMSA was performed using a commercially available gel shift kit (Panomics, Inc., Redwood City, CA, USA) according to the manufacturer's instructions. Briefly, 10 μg of nuclear extract were incubated with biotin end-labeled 22-mer double-stranded NF-κB oligonucleotide 5'-AGTTGAGG GGACTTTCCCAGGC-3' (underlined letters indicate NF-κB-binding site) for 30 min at 15°C. The specificity of NF-κB DNA binding was then determined by evaluating the effects of competition with a 33-fold unlabeled oligonucleotide. The DNA-protein complexes were then analyzed by electrophoresis on a 6% non-denaturing polyacrylamide gel and subsequently transferred onto a neutrally charged nylon membrane. The oligonucleotide on the membrane was then fixed using a UV crosslinker for 3 min, after which band detection was performed using the detection system provided with the kit.

**Measurement of PGE<sub>2</sub> synthesis.** PGE<sub>2</sub> synthesis was assessed using a commercially available PGE<sub>2</sub> competitive enzyme immunoassay kit (Amersham Biosciences Corp., Piscataway, NJ, USA). Briefly, 100 μl of supernatant from the culture medium and the standards were added to different wells on the goat anti-mouse IgG-coated microtiter plate provided with the kit. Mouse anti-PGE<sub>2</sub> antibody and peroxidase-conjugated PGE<sub>2</sub> were then added to each well, after which the plate was incubated at room temperature with shaking for 2 h. The wells were then drained and washed, after which 3,3',5,5'-tetramethylbenzidine/hydrogen peroxide solution was added. The plate was then incubated at room temperature with shaking for 30 min, after which the reaction was stopped by the addition of H<sub>2</sub>SO<sub>4</sub>. The absorbance of the content of each well was then measured at a wavelength of 450 nm.

**Determination of NO production.** To determine the effect of ulinastatin on NO production, the amount of nitrite in the supernatant was measured using a commercially available NO

detection kit (Intron, Inc., Seoul, Korea). After collection of 100 μl of supernatant, 50 μl of N1 buffer were added to each well, and the plate was then incubated at room temperature for 10 min. N2 buffer was then added, after which the plate was incubated at room temperature for 10 min. The absorbance of the content of each well was then measured at a wavelength of 540 nm and the nitrite concentration was calculated from a nitrite standard curve.

**Statistical analysis.** The results are presented as the means ± standard error of the mean (SEM). The data were analyzed by one-way ANOVA followed by Duncan's post hoc test using SPSS software. P<0.05 was considered to indicate a statistically significant difference.

## Results

**Effect of ulinastatin on the viability of BV2 mouse microglial cells.** To assess the cytotoxic effect of ulinastatin on BV2 mouse microglial cells, the cells were cultured with ulinastatin at final a concentration of 1, 10, 100, 1,000 and 10,000 U/ml for 24 h, after which MTT assay was conducted. Cells cultured in ulinastatin-free medium were used as the control. The viability of cells incubated with ulinastatin at concentrations of 1, 10, 100, 1,000 and 10,000 U/ml for 24 h was 96.50±0.94%, 97.22±1.03%, 95.00±1.41%, 92.45±1.38% and 56.96±1.13% of the control value, respectively. These results demonstrate that ulinastatin exerted no cytotoxic effects at concentrations <1,000 U/ml and that 10,000 U/ml of ulinastatin significantly reduced cell viability. Therefore, we used 10, 100 and 1,000 U/ml of ulinastatin for all subsequent experiments.

**Effect of ulinastatin on the mRNA expression of COX-2 and iNOS.** The levels of COX-2 and iNOS mRNA in ulinastatin treated cells were evaluated and then compared to the levels in the LPS-treated cells to determine the effects of ulinastatin on the expression of these genes. In the present study, the levels of COX-2 and iNOS mRNA in the control cells were set at 1.00.

The level of COX-2 mRNA was markedly increased to 4.61±0.78 following treatment with 2 μg/ml LPS for 24 h. However, these increased COX-2 mRNA levels decreased to 4.68±0.85, 3.50±0.58 and 1.76±0.97 in the cells that were pre-treated for 1 h with 10, 100 and 1,000 U/ml ulinastatin, respectively, and then treated with 2 μg/ml LPS for 24 h.

The level of iNOS mRNA following treatment with 2 μg/ml LPS for 24 h was markedly increased to 3.99±0.37. However, the levels of iNOS mRNA were only 3.24±0.31, 2.52±0.21 and 1.62±0.11 when the cells were pre-treated for 1 h with 10, 100 and 1,000 U/ml ulinastatin, respectively, and then treated with 2 μg/ml LPS for 24 h. These findings demonstrate that treatment with LPS enhanced COX-2 and iNOS mRNA expression in BV2 mouse microglial cells, and that pre-treatment with ulinastatin suppressed the LPS-induced COX-2 and iNOS mRNA expression (Fig. 1).

**Effect of ulinastatin on the protein expression of COX-2 and iNOS.** The protein levels of COX-2 and iNOS in the cells that were treated with ulinastatin were evaluated and compared to the levels in the control cells to determine the effects of ulinastatin on the expression of these proteins. In the present

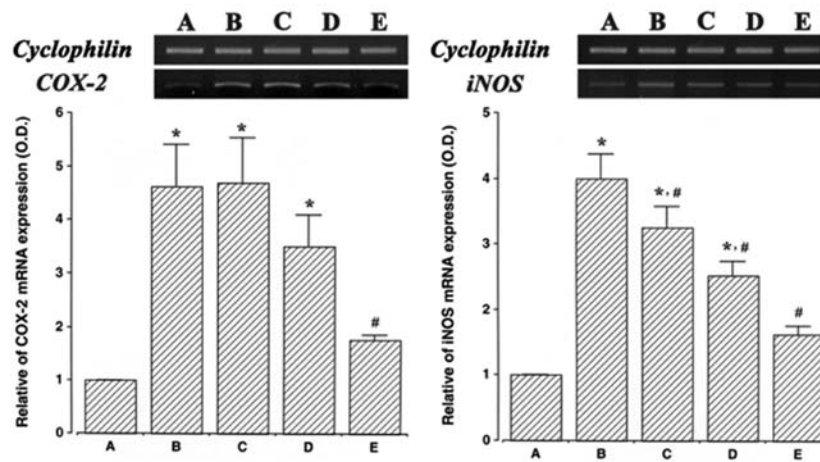


Figure 1. RT-PCR analysis of the mRNA levels of cyclooxygenase-2 (COX-2) and inducible nitric oxide synthase (iNOS). BV2 mouse microglial cells were pre-treated with ulinastatin at a concentration of 10, 100 and 1,000 U/ml for 1 h, and then treated with 2  $\mu$ g/ml lipopolysaccharide (LPS) for 24 h. Cyclophilin was used as the internal control. (A) Control group, (B) LPS-treated group, (C) LPS- and 10 U/ml ulinastatin pre-treated group, (D) LPS- and 100 U/ml ulinastatin pre-treated group, (E) LPS- and 1,000 U/ml ulinastatin pre-treated group. The results are presented as the means  $\pm$  standard error of the mean (SEM). \* $P$ <0.05 compared to the control group. # $P$ <0.05 compared to the LPS-treated group.

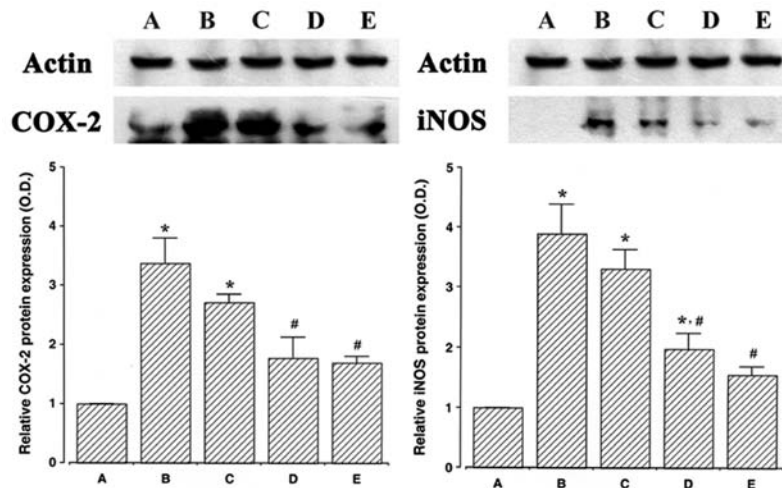


Figure 2. Western blot analysis of the protein levels of cyclooxygenase-2 (COX-2) and inducible nitric oxide synthase (iNOS). BV2 mouse microglial cells were pre-treated with ulinastatin at a concentration of 10, 100 and 1,000 U/ml for 1 h, and then treated with 2  $\mu$ g/ml lipopolysaccharide for 24 h. Actin was used as the internal control. (A) Control group, (B) LPS-treated group, (C) LPS- and 10 U/ml ulinastatin pre-treated group, (D) LPS- and 100 U/ml ulinastatin pre-treated group, (E) LPS- and 1,000 U/ml ulinastatin pre-treated group. The results are presented as the means  $\pm$  standard error of the mean (SEM). \* $P$ <0.05 compared to the control group. # $P$ <0.05 compared to the LPS-treated group.

study, the protein levels of COX-2 and iNOS in the control cells were set at 1.00.

The protein level of COX-2 markedly increased to  $3.37 \pm 0.41$  following treatment with 2  $\mu$ g/ml LPS for 24 h. However, the protein levels of COX-2 decreased to  $2.70 \pm 0.14$ ,  $1.77 \pm 0.35$  and  $1.69 \pm 0.11$  in the cells that were pre-treated for 1 h with 10, 100 and 1,000 U/ml of ulinastatin, respectively, and then treated with 2  $\mu$ g/ml LPS for 24 h.

Following treatment with 2  $\mu$ g/ml LPS for 24 h, the protein level of iNOS markedly increased to  $3.89 \pm 0.48$ . However, the protein levels of iNOS decreased to  $3.31 \pm 0.32$ ,  $1.98 \pm 0.26$  and  $1.54 \pm 0.14$  in the cells that were pre-treated with 10, 100 and 1,000 U/ml ulinastatin, respectively, and then treated with 2  $\mu$ g/ml LPS for 24 h. These results demonstrate that treatment with LPS enhanced COX-2 and iNOS protein expression in BV2 mouse microglial cells, and that pre-treatment with

ulinastatin suppressed the LPS-induced protein expression of COX-2 and iNOS (Fig. 2).

*Effect of ulinastatin on NF- $\kappa$ B protein in the nuclear fraction and I $\kappa$ B- $\alpha$  protein in the cytosolic fraction.* The protein levels of NF- $\kappa$ B and I $\kappa$ B- $\alpha$  were evaluated to determine the effects of ulinastatin on the expression of these proteins. In the present study, the protein levels of NF- $\kappa$ B and I $\kappa$ B- $\alpha$  in the control cells were set at 1.00.

The protein level of NF- $\kappa$ B in the nuclear fraction markedly increased to  $2.10 \pm 0.12$  following treatment with 2  $\mu$ g/ml LPS for 30 min. However, the protein levels of NF- $\kappa$ B in the nuclear fraction decreased to  $1.88 \pm 0.19$ ,  $1.26 \pm 0.10$  and  $1.17 \pm 0.12$  in the cells that were pre-treated for 1 h with 10, 100 and 1,000 U/ml ulinastatin, respectively, and then treated with 2  $\mu$ g/ml LPS.

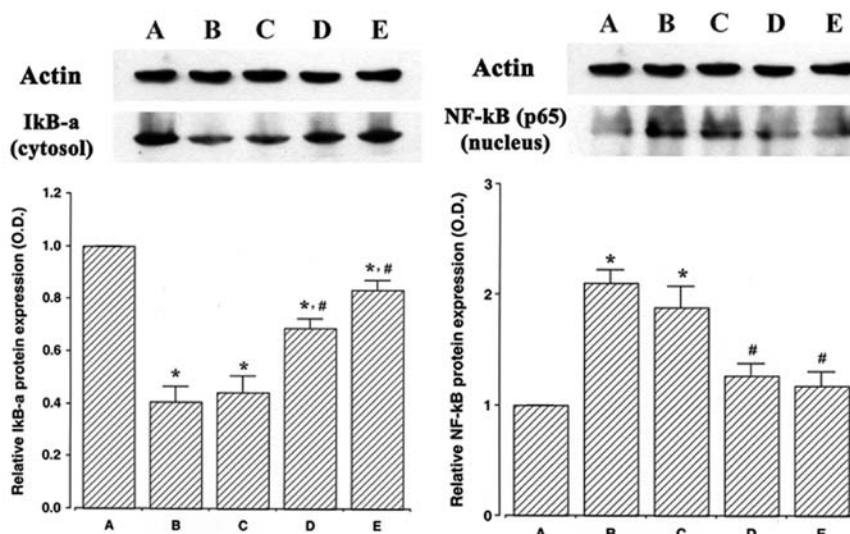


Figure 3. Western blot analysis of the protein levels of nuclear factor- $\kappa$ B (NF- $\kappa$ B) and inhibitory  $\kappa$ B- $\alpha$  (I $\kappa$ B- $\alpha$ ). BV2 mouse microglial cells were pre-treated for 1 h with ulinastatin at a concentration of 10, 100 and 1,000 U/ml, and then treated with 2  $\mu$ g/ml lipopolysaccharide (LPS) for 30 min. (A) Control group, (B) LPS-treated group, (C) LPS- and 10 U/ml ulinastatin pre-treated group, (D) LPS- and 100 U/ml ulinastatin pre-treated group, (E) LPS- and 1,000 U/ml ulinastatin pre-treated group. The results are presented as the means  $\pm$  standard error of the mean (SEM). \* $P$ <0.05 compared to the control group. # $P$ <0.05 compared to the LPS-treated group.

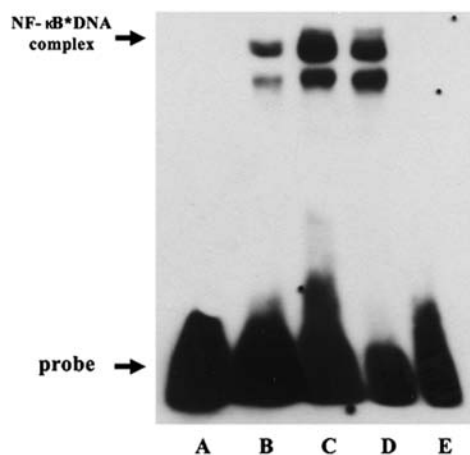


Figure 4. Analysis of nuclear factor- $\kappa$ B (NF- $\kappa$ B) binding by electrophoretic mobility gel shift assay (EMSA). BV2 mouse microglial cells were pre-treated for 1 h with ulinastatin at a concentration of 1,000 U/ml, and then treated with 2  $\mu$ g/ml lipopolysaccharide (LPS) for 30 min. Nuclear extracts were then analyzed for NF- $\kappa$ B binding by EMSA. The specificity of NF- $\kappa$ B DNA binding was examined by evaluating the effects of competition with the 33-fold unlabeled oligonucleotide. (A) Labeled NF- $\kappa$ B probe only with no sample, (B) labeled NF- $\kappa$ B probe with control group, (C) labeled NF- $\kappa$ B probe with LPS-treated group, (D) labeled NF- $\kappa$ B probe with the group that was pre-treated with 1,000 U/ml ulinastatin and then LPS, (E) LPS-treated with cold and labeled NF- $\kappa$ B probe.

The protein level of I $\kappa$ B- $\alpha$  in the cytosolic fraction markedly decreased to  $0.40 \pm 0.05$  following treatment with 2  $\mu$ g/ml LPS for 30 min. However, the protein levels of I $\kappa$ B- $\alpha$  in the cytosolic fraction increased to  $0.44 \pm 0.06$ ,  $0.68 \pm 0.03$  and  $0.83 \pm 0.03$  in the cells that were pre-treated for 1 h with 10, 100 and 1,000 U/ml of ulinastatin, respectively, and then treated with 2  $\mu$ g/ml LPS for 30 min. The results of this study demonstrate that treatment with LPS increased NF- $\kappa$ B protein expression in the nucleus and decreased I $\kappa$ B- $\alpha$  protein expression in the cytosol of BV2

mouse microglial cells, whereas pre-treatment with ulinastatin suppressed NF- $\kappa$ B protein expression and increased I $\kappa$ B- $\alpha$  protein expression (Fig. 3).

**Effect of ulinastatin on DNA binding activity of NF- $\kappa$ B.** To confirm the effect of ulinastatin on NF- $\kappa$ B activation, we evaluated the DNA binding activity of NF- $\kappa$ B using EMSA. Treatment with 2  $\mu$ g/ml LPS for 30 min increased the DNA binding activity of NF- $\kappa$ B. However, the LPS-induced DNA binding activity of NF- $\kappa$ B decreased in response to pre-treatment with 1,000 U/ml ulinastatin. These findings demonstrate that treatment with LPS enhanced the DNA binding activity of NF- $\kappa$ B in BV2 mouse microglial cells and that pre-treatment with ulinastatin suppressed the LPS-induced increase in the DNA binding activity of NF- $\kappa$ B (Fig. 4).

**Effect of ulinastatin on PGE<sub>2</sub> synthesis and NO production.** The results of a PGE<sub>2</sub> immunoassay revealed that the amount of PGE<sub>2</sub> present in the culture medium increased from  $26.58 \pm 0.82$  pg/ml to  $94.34 \pm 7.04$  pg/ml following 24 h of exposure to LPS. However, the levels of PGE<sub>2</sub> synthesis decreased to  $90.90 \pm 7.61$ ,  $69.27 \pm 4.15$ ,  $62.51 \pm 4.92$  and  $38.91 \pm 1.49$  pg/ml in the cells that were pre-treated for 1 h with 10, 100, 1,000 U/ml ulinastatin and 500  $\mu$ M acetylsalicylic acid (ASA), respectively, prior to treatment with 2  $\mu$ g/ml LPS for 24 h.

The results of the NO detection assay revealed that the concentration of nitrite increased from  $3.00 \pm 0.38$   $\mu$ M to  $19.97 \pm 0.93$   $\mu$ M following 24 h of exposure to LPS. However, the levels of NO production decreased to  $17.14 \pm 0.78$ ,  $16.15 \pm 0.81$ ,  $11.91 \pm 0.44$  and  $13.05 \pm 0.79$   $\mu$ M in the cells that were pre-treated for 1 h with 10, 100, 1,000 U/ml ulinastatin and 500  $\mu$ M ASA, respectively, prior to treatment with 2  $\mu$ g/ml LPS for 24 h.

These results demonstrate that LPS enhanced PGE<sub>2</sub> synthesis and NO production in BV2 mouse microglial cells and that pre-treatment with ulinastatin suppressed the LPS-induced PGE<sub>2</sub> synthesis and NO production (Fig. 5).

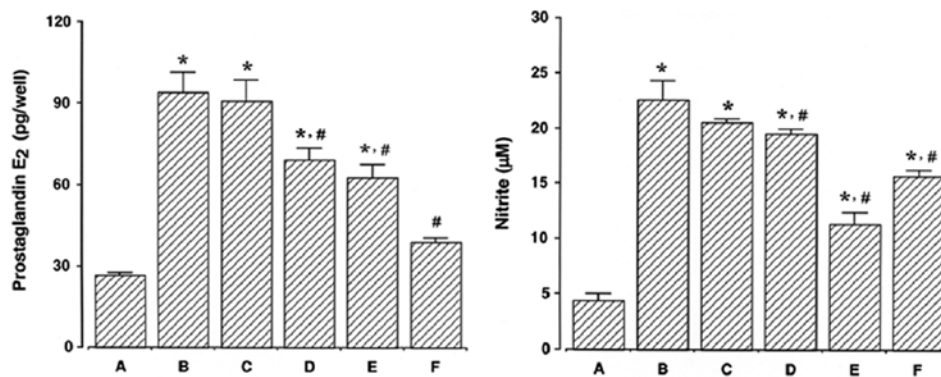


Figure 5. Measurement of prostaglandin E<sub>2</sub> (PGE<sub>2</sub>) synthesis and nitric oxide (NO) production in BV2 mouse microglial cells. BV2 mouse microglial cells were pre-treated with ulinastatin for 1 h at a concentration of 10, 100, and 1,000 U/ml, and then treated with 2 μg/ml lipopolysaccharide (LPS) for 24 h. Left panel, PGE<sub>2</sub> synthesis; right panel, NO production. (A) Control group, (B) LPS-treated group, (C) LPS- and 10 U/ml ulinastatin pre-treated group, (D) LPS- and 100 U/ml ulinastatin pre-treated group, (E) LPS- and 1,000 U/ml ulinastatin pre-treated group, (F) LPS- and 500 μM acetylsalicylic acid pre-treated group. The results are presented as the means ± standard error of the mean (SEM). \*P<0.05 compared to the control group. #P<0.05 compared to the LPS-treated group.

## Discussion

Organ protection is a routine therapy in patients with severe trauma, infection, and even multiple organ dysfunction syndrome. Urinary trypsin inhibitors have been widely used for the treatment of acute inflammatory disorders (22). A number of studies have reported that urinary trypsin inhibitors suppress the enhanced production of pro-inflammatory molecules such as prostaglandin H<sub>2</sub> synthase-2 (23), IL-8 (24) and TNF- $\alpha$  (25). Recently, Qiu *et al* (26) demonstrated that ulinastatin exerted protective effect against smoke inhalation-induced acute lung injury and the subsequent development of pulmonary fibrosis in rats. Pre-treatment with ulinastatin has also been shown to ameliorate oxidative injury in rats (27). Inflammation, which is a complex process that commences with a primary reaction in tissues, is involved in multiple pathologies, including arthritis, asthma, multiple sclerosis, colitis, inflammatory bowel disease and atherosclerosis. COX-2 and iNOS are 2 primary inflammatory markers produced by microglia in the CNS.

In the present study, pre-treatment with ulinastatin significantly suppressed LPS-induced COX-2 expression and PGE<sub>2</sub> synthesis in BV2 mouse microglial cells. A high level of COX-2 activity is closely associated with the occurrence of arthritis. In addition, it is well known that specific COX-2 inhibitors attenuate the symptoms of inflammation (28). PGE<sub>2</sub> is a major metabolite of the COX-2 pathway that has emerged as an important lipid mediator of inflammatory and immune regulatory processes (29).

As shown in the present study, pre-treatment with ulinastatin significantly inhibited LPS-induced iNOS expression as well as NO production in BV2 mouse microglial cells. During macrophage activation, iNOS has been shown to mediate NO-induced cell injury through the generation of reactive radicals, such as peroxynitrite (4). The excessive production of NO by iNOS has been implicated in a variety of pathological processes, including septic shock, rheumatoid arthritis and carcinogenesis (30,31). In addition, NO is known to modulate the activity of COX-2 in a cyclic guanosine monophosphate (cGMP)-independent manner, as well as to play a critical role in the release of PGE<sub>2</sub> by the direct activation of COX-2 (32). This synergistic induction of NO and PGE<sub>2</sub> is also related to

the overproduction of the earliest expressed pro-inflammatory cytokines (33,34).

The ubiquitous NF- $\kappa$ B signaling pathway plays an important role in the regulation of inflammation through the transcription of the COX-2, iNOS and cytokine genes (8). In this study, we investigated the DNA binding activity of NF- $\kappa$ B to determine whether the inhibition of COX-2 and iNOS is mediated by the NF- $\kappa$ B signaling pathway. Pre-treatment with ulinastatin significantly suppressed the LPS-induced nuclear translocation of NF- $\kappa$ B, and this inhibition corresponded to the inhibition of COX-2 and iNOS expression in BV2 mouse microglial cells. These findings are supported by previous studies, indicating that the blockage of NF- $\kappa$ B transcriptional activity suppresses COX-2 and iNOS expression and pro-inflammatory cytokine production (2,35,36). NF- $\kappa$ B is located in the cytoplasm as an inactive complex bound to I $\kappa$ B- $\alpha$ , and then it is degraded upon phosphorylation, after which it dissociates to produce activated NF- $\kappa$ B (37). The results from the present study indicate that ulinastatin blocks the LPS-induced translocation of NF- $\kappa$ B via the inhibition of the degradation of I $\kappa$ B- $\alpha$ . The blockage of NF- $\kappa$ B activation has potential as a therapeutic modality for the treatment of inflammatory bowel disease and arthritis (38,39). The inhibitory effect of ulinastatin on NF- $\kappa$ B signal transduction has been shown to suppress the proliferation and induce the apoptosis of human breast cancer cells (40).

In this study, we demonstrated that ulinastatin exerts analgesic and anti-inflammatory effects by suppressing COX-2 and iNOS expression, which results in the inhibition of PGE<sub>2</sub> synthesis and NO production. The present study also reveals that the analgesic and anti-inflammatory effects of ulinastatin involve the blockage of NF- $\kappa$ B activation in LPS-stimulated BV2 mouse microglial cells. These results suggest that the analgesic and anti-inflammatory effects of ulinastatin possibly occur via the suppression of COX-2 and iNOS expression through the downregulation of NF- $\kappa$ B activity.

## Acknowledgements

This study was supported by the Program of Kyung Hee University for the Young Researcher of Medical Science in 2007 (KHU-20071478).

## References

- Liu B and Hong JS: Role of microglia in inflammation-mediated neurodegenerative diseases: mechanisms and strategies for therapeutic intervention. *J Pharmacol Exp Ther* 304: 1-7, 2003.
- Moon DO, Choi YH, Kim ND, Park YM and Kim GY: Anti-inflammatory effects of  $\beta$ -lapachone in lipopolysaccharide-stimulated BV2 microglia. *Int Immunopharmacol* 7: 506-514, 2007.
- Kubes P and McCafferty DM: Nitric oxide and intestinal inflammation. *Am J Med* 109: 150-158, 2000.
- Lee AK, Sung SH, Kim YC and Kim SG: Inhibition of lipopolysaccharide-inducible nitric oxide synthase, TNF- $\alpha$  and COX-2 expression by sauchinone effects on I- $\kappa$ B $\alpha$  phosphorylation, C/EBP and AP-1 activation. *Br J Pharmacol* 139: 11-20, 2003.
- Palladino MA, Bahjat FR, Theodorakis EA and Moldawer LL: Anti-TNF- $\alpha$  therapies: the next generation. *Nat Rev Drug Discov* 2: 736-746, 2003.
- Kalmar B, Kittel A, Lemmens R, Kornyei Z and Madarasz E: Cultured astrocytes react to LPS with increased cyclooxygenase activity and phagocytosis. *Neurochem Int* 38: 453-461, 2001.
- Park HJ, Kim IT, Won JH, Jeong SH, Park EY, Nam JH, Choi J and Lee KT: Anti-inflammatory activities of *ent-16 $\alpha$ H,17-hydroxykauran-19-oic acid* isolated from the roots of *Siegesbeckia pubescens* are due to the inhibition of iNOS and COX-2 expression in RAW 264.7 macrophages via NF- $\kappa$ B inactivation. *Eur J Pharmacol* 558: 185-193, 2007.
- Surh YJ, Chun KS, Cha HH, Han SS, Keum YS, Park KK and Lee SS: Molecular mechanisms underlying chemopreventive activities of anti-inflammatory phytochemicals: down-regulation of COX-2 and iNOS through suppression of NF- $\kappa$ B activation. *Mutat Res* 480-481: 243-268, 2001.
- Bredt DS and Snyder SH: Nitric Oxide: a physiologic messenger molecule. *Annu Rev Biochem* 63: 175-195, 1994.
- Xie Q and Nathan C: The high-output nitric oxide pathway: role and regulation. *J Leukoc Biol* 56: 576-582, 1994.
- Lappas M, Permezel M, Georgiou HM and Rice GE: Nuclear factor kappa B regulation of proinflammatory cytokines in human gestational tissues in vitro. *Biol Reprod* 67: 668-673, 2002.
- Karin M: The beginning of the end: I $\kappa$ B kinase (IKK) and NF- $\kappa$ B activation. *J Biol Chem* 274: 27339-27342, 1999.
- Maciejewski R, Burdan F, Burski K, Madej B, Ziemiakowicz R, Dabrowski A and Wallner G: Selected biochemical parameters and ultrastructural picture of pancreas due to Ulinastatin treatment of experimental acute pancreatitis. *Exp Toxicol Pathol* 56: 305-311, 2005.
- Tani T, Aoki H, Yoshioka T, Lin KJ and Kodama M: Treatment of septic shock with a protease inhibitor in a canine model: a prospective, randomized, controlled trial. *Crit Care Med* 21: 925-930, 1993.
- Masuda T, Sato K, Noda C, Ikeda KM, Matsunaga A, Ogura MN, Shimizu K, Nagasawa H, Matsuyama N and Izumi T: Protective effect of urinary trypsin inhibitor on myocardial mitochondria during hemorrhagic shock and reperfusion. *Crit Care Med* 31: 1987-1992, 2003.
- Yano T, Anraku S, Nakayama R and Ushijima K: Neuroprotective effect of urinary trypsin inhibitor against focal cerebral ischemia-reperfusion injury in rats. *Anesthesiology* 98: 465-473, 2003.
- Shin IW, Jang IS, Lee SM, Park KE, Ok SH, Sohn JT, Lee HK and Chung YK: Myocardial protective effect by ulinastatin via an anti-inflammatory response after regional ischemia/reperfusion injury in an in vivo rat heart model. *Korean J Anesthesiol* 61: 499-505, 2011.
- Molitor-Erdene P, Okajima K, Isobe H, Uchiba M, Harada N and Okabe H: Urinary trypsin inhibitor reduces LPS-induced hypotension by suppressing tumor necrosis factor- $\alpha$  production through inhibition of Egr-1 expression. *Am J Physiol Heart Circ Physiol* 288: H1265-H1271, 2005.
- Tanaka Y, Maehara S, Sumi H, Toki N, Moriyama S and Sasaki K: Purification and partial characterization of two forms of urinary trypsin inhibitor. *Biochim Biophys Acta* 705: 192-199, 1982.
- Kanai T, Ishiwata T, Kobayashi T, Sato H, Takizawa M, Kawamura Y, Tsujimoto H, Nakatani K, Ishibashi N, Nishiyama M, Hatai Y, Asano Y, Kobayashi T, Takeshita S and Nonoyama S: Ulinastatin, a urinary trypsin inhibitor, for the initial treatment of patients with Kawasaki disease: a retrospective study. *Circulation* 124: 2822-2828, 2011.
- Gao C, Li R and Wang S: Ulinastatin protects pulmonary tissues from lipopolysaccharide-induced injury as an immunomodulator. *J Trauma Acute Care Surg* 72: 169-176, 2012.
- Inoue K, Takano H, Shimada A, Yanagisawa R, Sakurai M, Yoshino S, Sato H and Yoshikawa T: Urinary trypsin inhibitor protects against systemic inflammation induced by lipopolysaccharide. *Mol Pharmacol* 67: 673-680, 2005.
- Zaitzu M, Hamasaki Y, Tashiro K, Matsuo M, Ichimaru T, Fujita I, Tasaki H and Miyazaki S: Ulinastatin, an elastase inhibitor, inhibits the increased mRNA expression of prostaglandin H<sub>2</sub> synthase-type 2 in Kawasaki disease. *J Infect Dis* 181: 1101-1109, 2000.
- Nakamura H, Abe S, Shibata Y, Sata M, Kato S, Saito H, Hino T, Takahashi H and Tomoike H: Inhibition of neutrophil elastase-induced interleukin-8 gene expression by urinary trypsin inhibitor in human bronchial epithelial cells. *Int Arch Allergy Immunol* 112: 157-162, 1997.
- Aosasa S, Ono S, Mochizuki H, Tsujimoto H, Ueno C and Matsumoto A: Mechanism of the inhibitory effect of protease inhibitor on tumor necrosis factor alpha production of monocytes. *Shock* 15: 101-105, 2001.
- Qiu X, Ji S, Wang J, Li H, Xia T, Pan B, Xiao S and Xia Z: The therapeutic efficacy of Ulinastatin for rats with smoking inhalation injury. *Int Immunopharmacol* 14: 289-295, 2012.
- Xu CE, Zhang MY, Zou CW and Guo L: Evaluation of the pharmacological function of ulinastatin in experimental animals. Evaluation of the pharmacological function of ulinastatin in experimental animals. *Molecules* 17: 9070-9080, 2012.
- Crofford LJ, Lipsky PE, Brooks P, Abramson SB, Simon LS and van de Putte LB: Basic biology and clinical application of specific cyclooxygenase-2 inhibitors. *Arthritis Rheum* 43: 4-13, 2000.
- Hinz B, Brune K and Pahl A: Prostaglandin E<sub>2</sub> upregulates cyclooxygenase-2 expression in lipopolysaccharide-stimulated raw 264.7 macrophages. *Biochem Biophys Res Commun* 272: 744-748, 2000.
- Ohshima H and Bartsch H: Chronic infections and inflammatory processes as cancer risk factors: possible role of nitric oxide in carcinogenesis. *Mutat Res* 305: 253-264, 1994.
- Salerno L, Sorrenti V, Di Giacomo C, Romeo G and Siracusa MA: Progress in the development of selective nitric oxide synthase (NOS) inhibitors. *Curr Pharm Des* 8: 177-200, 2002.
- Salvemini D, Misko TP, Masferrer JL, Seibert K, Currie MG and Needleman P: Nitric oxide activates cyclooxygenase enzymes. *Proc Natl Acad Sci USA* 90: 7240-7244, 1993.
- Jun CD, Choi BM, Kim HM and Chung HT: Involvement of protein kinase C during taxol-induced activation of murine peritoneal macrophages. *J Immunol* 154: 6541-6547, 1995.
- White KE, Ding Q, Moore BB, Peters-Golden M, Ware LB, Matthay MA and Olman MA: Prostaglandin E<sub>2</sub> mediates IL-1 $\beta$ -related fibroblast mitogenic effects in acute lung injury through differential utilization of prostanoid receptors. *J Immunol* 180: 637-646, 2008.
- Petrova TV, Akama KT and Van Eldik LJ: Cyclopentenone prostaglandins suppress activation of microglia: down-regulation of inducible nitric oxide synthase by 15-deoxy- $\Delta^{12,14}$ -prostaglandin J<sub>2</sub>. *Proc Natl Acad Sci USA* 96: 4668-4673, 1999.
- Ye SM and Johnson RW: Regulation of interleukin-6 gene expression in brain of aged mice by nuclear factor  $\kappa$ B. *J Neuroimmunol* 117: 87-96, 2001.
- Baeuerle PA and Baltimore D: NF- $\kappa$ B: ten years after. *Cell* 87: 13-20, 1996.
- Dijkstra G, Moshage H and Jansen PL: Blockade of NF- $\kappa$ B activation and donation of nitric oxide: new treatment options in inflammatory bowel disease? *Scand J Gastroenterol Suppl* 236: 37-41, 2002.
- Simmonds RE and Foxwell BM: Signalling, inflammation and arthritis: NF- $\kappa$ B and its relevance to arthritis and inflammation. *Rheumatology* 47: 584-590, 2008.
- Wang H, Sun X, Gao F, Zhong B, Zhang YH and Sun Z: Effect of ulinastatin on growth inhibition, apoptosis of breast carcinoma cells is related to a decrease in signal conduction of JNK-2 and NF- $\kappa$ B. *J Exp Clin Cancer Res* 31: 2, 2012.